A Luminescent β-Cyclodextrin-Based $Ru(phen)_3$ Complex as DNA Compactor, Enzyme Inhibitor, and Translocation Tracer

Yu Liu,[†,*] Yong Chen,[†] Zhong-Yu Duan,[†] Xi-Zeng Feng,[‡,*] Sen Hou,[‡] Chen Wang,[§] and Rui Wang[§]

[†]Department of Chemistry, State Key Laboratory of Elemento-Organic Chemistry, Nankai University, Tianjin 300071, P. R. China, [‡]College of Life Science, Nankai University, Tianjin 300071, P. R. China, and [§]National Center for Nanoscience and Technology, Beijing, 100080, P. R. China

ABSTRACT A β-cyclodextrin-based $Ru(phen)_3$ complex (**1**) has been synthesized and exhibits good luminescent behavior. Atomic force microscopic and scanning electron microscopic studies show that **1** can induce the aggregation of originally circular DNA to toroidal or spherical shapes. The morphology of these DNA aggregates changes following a pathway of naked circular DNA → toroid with gaps → solid toroid → spherical aggregate, depending on the different 1/DNA (w/w) ratios, and their average diameters vary from the nanometer to micrometer scale. Owing to its capability of inducing the aggregation of DNA, **1** can be used as an inhibitor for DNA topoisomerase and DNA cleavage enzymes. Further studies by means of fluorescence microscopy indicate that **1** can also efficiently trace the translocation of DNA into 293T cells (the human embryonic kidney cell line). These observations consequently establish **1** as not only a potential DNA carrier but also a fluorescent DNA probe.

KEYWORDS: AFM · cyclodextrin · DNA · enzyme inhibitor · fluorescence probe · translocation

Owing to their photochemical, electrochemical, and magnetic properties[1–9] as well as their ability to interact with DNA,[10–15] polypyridine−ruthenium complexes have increasingly attracted the interest of chemists and biologists and have been successfully applied in many fields of material and biological science, such as solar/electrical energy conversation, long-range electron and energy transfer, molecular electronic devices, self-assembly processes, DNA photoprobes, *etc*. On the other hand, cyclodextrins (CDs), composed of six, seven, or eight D-glucopyranose units, possess truncated cone-shaped hydrophobic cavities which are capable of binding various organic, inorganic, and biological substrates to form supramolecular species.[16] Due to these properties, CDs have been extensively used as carriers and solubilizers for many biological and medicinal molecules.[17–19] The groups of Asuncion[20,21] and Schneider[22] reported that anthracene-modified CDs could be used as chemically switched DNA intercalators.

Herein, to combine the solubilization ability of CDs and the DNA-interaction properties of polypyridine−ruthenium complexes, we prepared a water-soluble HOP-β-CD/$Ru(phen)_2$ complex (**1**) from 2-(4′-hydroxyphenyl)imidazo[*f*]1,10-phenanthroline-modified β-CD (HOP-β-CD) and $Ru(phen)Cl_2$ (Scheme 1). Benefiting from the fascinating functions of the polypyridine−ruthenium unit, **1** exhibits the significant abilities to induce the aggregation of DNA through a process of free DNA → toroid aggregates (nanometer scale) → spherical aggregates (micrometer scale), inhibit the DNA topoisomerase and DNA cleavage enzymes, and trace the translocation of DNA into cells, which are fully characterized by means of atomic force microscopic (AFM), scanning electron microscopic (SEM), and fluorescence microscopic studies as well as agarose gel electrophoresis assays.

RESULTS AND DISCUSSION

Synthesis and Characterization. **1** was synthesized in a satisfactory yield (70%) by the reaction of HOP-β-CD with $Ru(phen)Cl_2$. Besides the elemental analysis and mass spectrum data, UV–vis and FT-IR spectra also provide evidence for the formation of **1**. The absorption maximum of the HOP group at 280 nm in the UV–vis spectrum of HOP-β-CD red-shifts to 285 nm in the UV–vis spectrum of **1**. Moreover, a new absorption at 458 nm, assigned to the metal–ligand charge-transfer (MLCT) band, is also observed in the UV–vis spectrum of **1**. In the FT-IR spectrum of **1**, the vibration band assigned to the phenanthroline group in HOP

*Address correspondence to yuliu@nankai.edu.cn, xzfeng@nankai.edu.cn.

Received for review July 4, 2007 and accepted October 22, 2007.

Published online November 9, 2007. 10.1021/nn7000849 CCC: $37.00

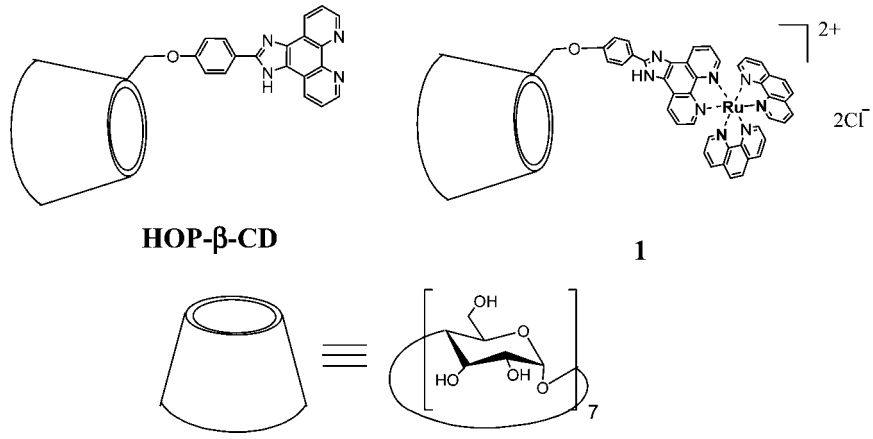

Scheme 1. Molecular structures of HOP-β-CD and 1.

shifts to the high-wavenumber region as compared with that of uncoordinated HOP-β-CD (from 1351 to 1363 cm^{-1}). These results jointly confirm the conversation of HOP-β-CD to a Ru(II)-coordinated species.

Circular dichroism spectroscopy is widely employed to elucidate the conformation of chiral compounds.[23,24] Herein, to examine the original conformation of **1** in aqueous solution, its circular dichroism spectrum was obtained at a concentration of 2.0×10^{-5} mol dm^{-3} and compared with that of HOP-β-CD. In Figure 1, the circular dichroism spectrum of HOP-β-CD shows one negative Cotton effect peak at 218 nm ($\Delta\epsilon = -1.91$ M^{-1} cm^{-1}) and one positive Cotton effect peak at 314 nm ($\Delta\epsilon = 4.35$ M^{-1} cm^{-1}). However, the circular dichroism spectrum of **1** gives several positive Cotton effect peaks at 212 nm ($\Delta\epsilon = 1.72$ M^{-1} cm^{-1}), 237 nm ($\Delta\epsilon = 1.08$ M^{-1} cm^{-1}), 276 nm ($\Delta\epsilon = 2.20$ M^{-1} cm^{-1}), and 308 nm ($\Delta\epsilon = 2.68$ M^{-1} cm^{-1}). According to the generally accepted empirical rule for the circular dichroism spectra of β-CD derivatives,[25,26] the sign of induced circular dichroism (ICD) signals depends mainly on the orientation of the transition dipole moment of the chromophore with respect to the C_7 axis of β-CD. If the chromophore is located inside the β-CD cavity or perched on the edge of the β-CD cavity, its electronic transition parallel to the β-CD axis gives a positive ICD signal, whereas perpendicular transition gives a negative signal, but this situation is reversed for a guest located outside the CD cavity. Therefore, we can deduce that the HOP group in HOP-β-CD is located inside the β-CD cavity or perched on the edge of β-CD cavity, but it is at the exterior of the β-CD cavity after coordination with Ru(II). This conformational change will be favorable for the association of the $Ru(phen)_2 \cdot$HOP unit in **1** with DNA.

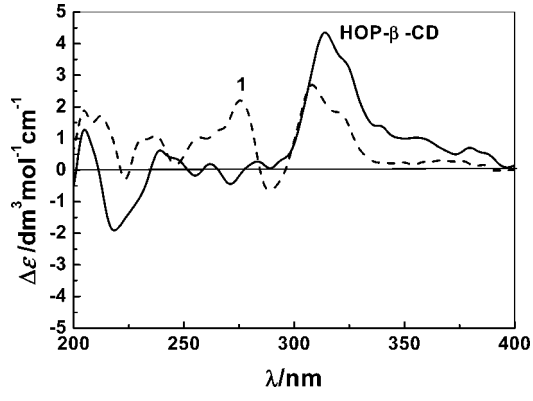

Figure 1. Circular dichroism spectra of HOP-β-CD and 1 (2.0×10^{-5} mol dm^{-3}) in Tris-HCl buffer solution (pH 7.20, 10 mM).

Benefiting from the fascinating photophysical property of the polypyridine−ruthenium(II) unit, **1** displays a significant luminescent behavior, which can be readily observed through fluorescence lifetime experiments using the time-correlated single-photon-counting technique. Besides a short fluorescence lifetime, $\tau_S =$ 1.2 ns (relative quantum yield = 0.037), **1** gives a quite long fluorescence lifetime, $\tau_L = 542$ ns (relative quantum yield = 0.963), assigned to the luminescence of the $Ru(phen)_2 \cdot$HOP unit. These results demonstrate a good photophysical property of **1**, which is important for its application in photophysics, photochemistry, and photobiology.

DNA Aggregation. The DNA interaction abilities of **1** are investigated by means of AFM and SEM experiments (Figure 2). The essential DNA used in these studies is the pEGFP-C2 plasmid DNA. Generally, this DNA exists as a mixture of circular supercoiled DNA (form I) and relaxed circular DNA (form II) arising from single-strand cleavage. Figure 2a shows a typical AFM image of naked pEGFP-C2 DNA (4.7 kb) on the mica surface, similar to that of naked Φx174 RFII dsDNA reported by Larson *et al.*[27] Most DNA molecules are circular or quasi-circular, and their length is measured to be *ca.* 1.56 μm, which is basically consistent with the calculated length (1.589 μm) of pEGFP-C2 DNA. At a low **1**/DNA (w/w) ratio (**1**/DNA ratio = 0.6), the circular or quasi-circular DNA first changes to loose toroids with gaps with an average diameter of *ca.* 735 nm (Figure 2b), accompanied by the obvious broadening of the DNA chain (bright lines in Figure 2b). After increasing the **1**/DNA ratio to 6, the originally loose toroids turn tense to some extent, and their average diameter decrease to *ca.* 700 nm (Figure 2c). This AFM image is similar to that of DNA condensates induced by spermidine.[28] When the **1**/DNA ratio increases to 120, the tense DNA toroids with gaps convert to solid toroids with an average diameter of *ca.* 475 nm (Figure 2d). At a higher **1**/DNA ratio up to 200, the solid toroids further convert to spherical aggregates on the micrometer scale. These phenomena conse-

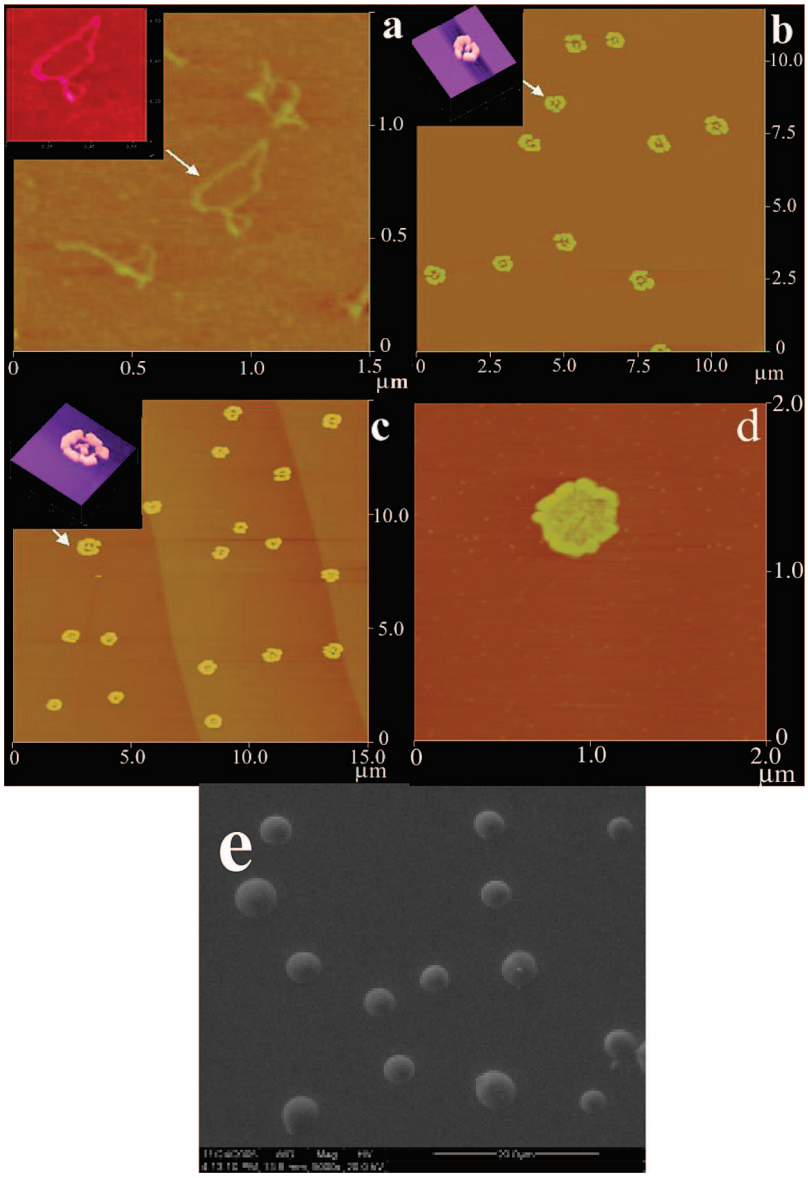

Figure 2. AFM images of (a) free DNA (0.075 ng/μL) (inset, enlarged image), (b) DNA (0.075 ng/μL) + 1 (0.045 ng/μL) (inset, 3D mode), (c) DNA (0.075 ng/μL) + 1 (0.45 ng/μL) (inset, 3D mode), and (d) DNA (0.075 ng/μL) + 1 (9 ng/μL) (inset, 3D mode). (e) SEM image of DNA (7.5 ng/μL) + 1 (1500 ng/μL).

quently validate the satisfactory DNA aggregation ability of **1**.

Enzyme Inhibition. Possessing a significant capability of inducing the aggregation of DNA, **1** also exhibits good inhibition abilities against some DNA enzymes such as *Hind*III and topoisomerase I. *Hind*III is a common restriction enzyme *in vivo*, which can specifically cleave closed supercoiled DNA (form I DNA) and nicked circular DNA (form II DNA) into linear DNA (form III DNA). Figure 3 illustrates the electrophoresis assay of pEGFP-C2 DNA at various **1**/DNA ratios in the presence of *Hind*III, with parent pEGFP-C2 DNA used as a control sample. In Figure 3, in the presence of *Hind*III, all of form I and form II DNA are cleaved to form III DNA when the **1**/DNA ratio is lower than 40. If the **1**/DNA ratio is increased beyond 40, the activity of the DNA restriction enzyme *Hind*III is gradually inhibited, and it is abolished when the **1**/DNA ratio reaches 200.

In addition, the inhibition ability of **1** against topoisomerase I, a commercial DNA topoisomerase, is also examined. Topoisomerase has been identified as an important biochemical target in chemotherapy and microbial infections. DNA topoisomerases are cellular enzymes that are intricately involved in the topographic structure of DNA transcription and mitosis[29] and can transform DNA from tense style to loose style. In Figure 4, **1** gives little to high antitopoisomerase activities with increasing the **1**/DNA ratios. That is, **1** shows no appreciable antitopoisomerase activity at a **1**/DNA ratio below 20, but it gives a significant antitopoisomerase activity (lowering the content of loose DNA from 99% to 72%) when the **1**/DNA ratio is increased to 60. These results are consistent with literature reports for $[Ru(\kappa^3\text{-L})(EPh_3)_2Cl]^+$ complex (E = P, As; L = 2,4,6-tris(2-pyridyl)-1,3,5- triazine)[11] and $[Ru(phen)_2(qdppz)]^{2+}$ complex (qdppz = naphtha[2,3-*a*]dipyrido[3,2-*h*:2′,3′-*f*]phenazine-5,18-dione),[12] which demonstrated that the aromatic ruthenium complexes showed good antitopoisomerase activities for pBR 322 DNA.

A possible reason for the efficient inhibition of **1** against topoisomerase I and *Hind*III may be the DNA aggregation induced by **1**. Generally, the interactions of enzyme with DNA depend upon the availability of enzyme binding sites in DNA. At low **1**/DNA ratios, DNA only forms loose aggregates (toroid with gaps), and there are still a number of DNA binding sites in these loose structures accessible for enzymes. However, at high **1**/DNA ratios, DNA forms compact aggregates (solid toroid or spherical aggre-

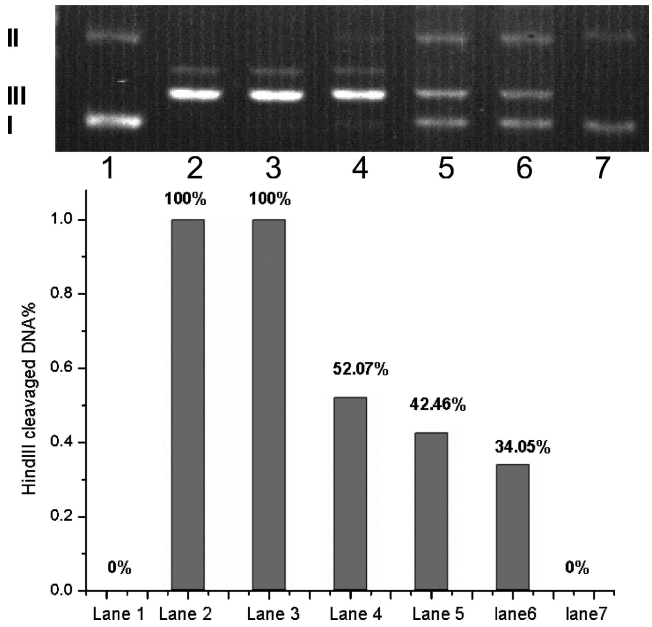

Figure 3. Agarose gel electrophoresis assay to investigate the inhibition ability of 1 against *Hin*dIII using plasmid pEGFP-C2 DNA (7.5 ng/μL in 1 mM EDTA/10 mM Tris buffer, pH 8.0). Lane 1, DNA alone; lane 2, DNA + *Hin*dIII; lanes 3–7, DNA + *Hin*dIII + 1 ([1] = 150, 300, 450, 600, and 1500 ng/μL, *i.e.*, 0.074, 0.147, 0.221, 0.295, and 0.737 mM from lane 3 to lane 7). All of the samples were incubated in the dark for 1 h. Samples 2–7 were then incubated with *Hin*dIII for 15 min, according to the protocols recommended by the supplier.

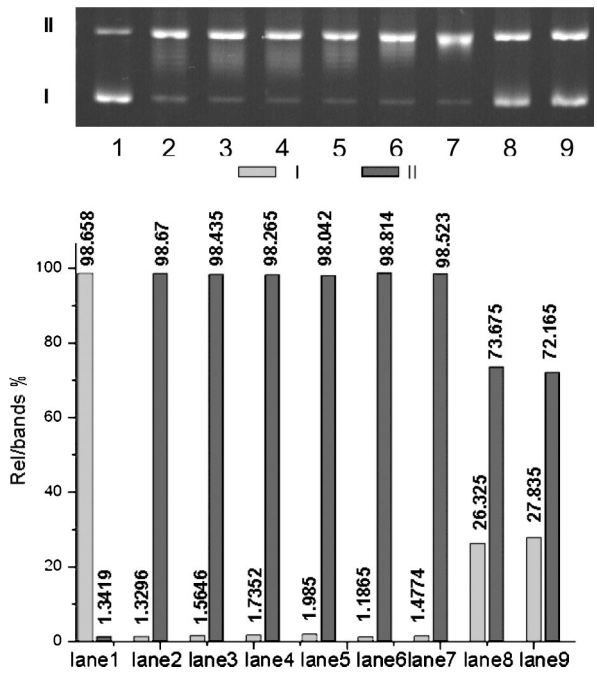

Figure 4. Agarose gel electrophoresis assay to investigate the inhibition ability of 1 against topomerase I using plasmid pEGFP-C2 DNA (7.5 ng/μL in 1 mM EDTA/10 mM Tris buffer, pH 8.0). Lane 1, DNA alone; lane 2, DNA + *Hin*dIII; lanes 3–9, DNA + topomerase I + 1 ([1] = 7.5, 22.5, 37.5, 52.5, 150, 300, and 450 ng/μL, *i.e.*, 0.0037, 0.011, 0.018, 0.026, 0.074, 0.147, and 0.221 mM from lane 3 to lane 9). All the samples were incubated in the dark for 1 h. Samples in lanes 2–9 were the incubated with topomerase I for 15 min, according to the protocols recommended by the supplier.

gate), which makes the binding site inaccessible and thus protects DNA from the digestion of enzymes.

Translocation Tracing. Significantly, **1** can also trace the translocation of DNA into cells due to its good luminescence property. In the DNA translocation experiment, **1** and pEGFP-C2 DNA were mixed and kept in the dark for 1 h, and then the **1**/DNA mixture was added into routinely cultured 293T cells. After 48 h, the DNA translocation efficiency was measured by means of fluorescence microscopy. Figure 5 shows the fluorescence microscopic images of the nonluminescent 293T cells in the presence of **1**/DNA mixtures and the corresponding phase contrast images, where the place with cells in the well is saffron and the place without cells is dark under fluorescence microscope. As can be seen in Figure 5b, nearly all of cells are luminescent under fluorescence microscope, indicating a quite high DNA translocation efficiency of **1**. In the control experiments, the 293T cells did not luminesce in the presence of pEGFP-C2 DNA but barely luminesce in the presence of **1** under the same conditions. These results demonstrate that **1** can be used as not only a gene carrier but also an efficient luminescent probe for the DNA translocation. It should be noteworthy that, as seen from Figure 5c,d, the luminescent **1**/DNA system is located mainly in the cytoplasm, but not karyon. A possible reason may be that the **1**-induced DNA aggregates are too large to be transported through the karyotheca.

CONCLUSION

In conclusion, a luminescent HOP-β-CD/$Ru(phen)_2$ complex has been synthesized and displays a satisfactory capability of inducing the aggregation of DNA, inhibiting some DNA enzymes, such as DNA topoisomerase and DNA restriction enzymes, and tracing the translocation of DNA into cells. Therefore, it can be used not only as a potential DNA carrier but also as a luminescent DNA probe. Owing to these advantages, **1** may be potentially applicable in many fields of pharmaceutical chemistry and biological technology. On the other hand, in the **1**-mediated DNA translocation process, the β-CD cavity of **1**, which has a good capability to accommodate hydrophobic molecules, is unoccupied. Therefore, **1** may also have the potential to carry some active drug molecules, many of which are usually hydrophobic and difficult to enter cells, into cells. This potential enables **1** as a possible drug carrier for *in vivo* therapy. Studies on the translocation of **1**/drug/DNA ternary systems into cells are still in progress.

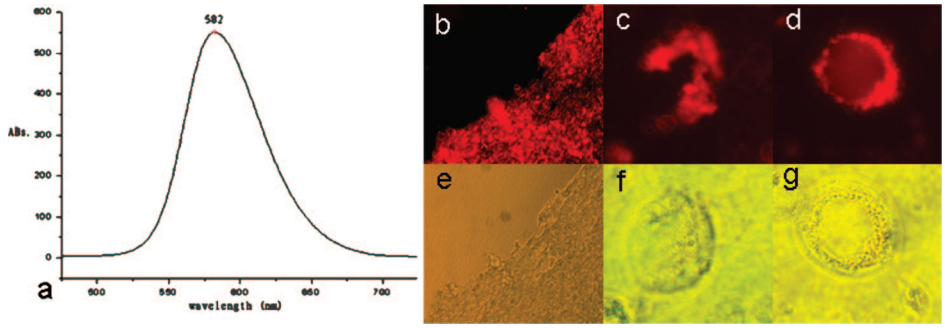

Figure 5. (a) Fluorescence spectrum of 1 (excited at 458 nm). (b) Fluorescence microscopic image of natural cultured 293T cells in the presence of 1/DNA mixtures. (c,d) Enlargements of the images in panel b. (e−g) Phase contrast images corresponding to panels b−d.

METHODS

General. 2-(4′-Hydroxyphenyl)imidazo[*f*]1,10-phenanthroline-modified β-CD[30] (HOP-β-CD) and Ru(phen)Cl_2[31] were prepared according to reported procedures. NMR spectra were recorded on a Varian Mercury 300 spectrometer in D_2O. Elemental analyses were performed on a Perkin-Elmer-2400C instrument. FT-IR spectra were recorded on a Shimadzu Bio-Rad FTS 135 instrument. SEM images were recorded on a HITACHI S-3500N scanning electron microscope. Circular dichroism and UV–vis spectra were recorded respectively in a conventional quartz cell (light path 10 mm) on a JASCO J-715S spectropolarimeter and on a Shimadzu UV-2401PC spectrophotometer equipped with a PTC-348WI temperature controller to keep the temperature at 25 °C. Fluorescence spectra in aqueous solution were measured in a conventional rectangular quartz cell (10 × 10 × 45 mm) at 25 °C on a JASCO FP-750 spectrometer equipped with a constant-temperature water bath, with excitation and emission slits width of 5 nm. Tris(hydroxymethyl)aminomethane and HCl were dissolved in distilled, deionized water to make a 10 mM Tris-HCl buffer solution of pH 7.20, which was used as solvent in all spectral measurements. Tapping-mode atomic force microscopy studies were performed on a Nanoscope IIIa AFM instrument (Veeco Metrology, USA) under ambient conditions, and commercial Si tips were used in all the experiments. The plasmid DNA solution was diluted with deionized water to appropriate concentration. The agglomerate solution was prepared by adding a solution of **1** (5 μL) to a solution of plasmid DNA (5 μL). After 30 min (at room temperature, dark environment), 2.5 μL of the mixture was dispersed on freshly cleaved mica.

Synthesis of 1. A mixture of HOP-β-CD (50 mg, 0.03 mmol) and Ru(phen)$_2Cl_2$ (16 mg, 0.03 mmol) was refluxed in 15 mL of EtOH−H_2O (v/v = 1:1) for 18 h. The obtained orange solution was poured into acetone (150 mL), and the precipitate was isolated by filtration. The crude product was purified on a Sephadex G-25 column using distilled, deionized water as an eluent and dried *in vacuo* to give **1** (46 mg, 70% yield). ESI-MS: *m/z* 945.5 [M − 2Cl]$^{2+}$. FT-IR (KBr): ν/cm^{-1} 3383, 3064, 2925, 1650, 1612, 1578, 1558, 1539, 1521, 1480, 1455, 1363, 1247, 1153, 1079, 1032, 944, 845, 809, 744, 722, 667, 583, 529, 460. UV–vis (H_2O): λ_{max} (ε) 458 nm (1.44 × 10^4 M^{-1} cm^{-1}), 285 nm (9.27 × 10^4 M^{-1} cm^{-1}). Anal. Calcd for $C_{85}H_{97}O_{35}N_8RuCl_2 \cdot 4H_2O$: C, 50.17; H, 5.20; N, 5.51. Found: C, 50.38; H, 5.46; N, 5.61.

Plasmid DNA Purification. Plasmid DNA pEGFP-C2 (4.7kb) was purified from *E. coli* DH5α using Wizard Plasmid DNA Purification System (catalog no. A2160, Promega). The concentration of plasmid DNA was measured through spectrophotometric analysis using a DU-7 spectrophotometer (Beckman). DNA was kept in TE buffer (10 mmol/L Tris-HCl, 1 mmol/L EDTA, pH 8.0).

Inhibition of *Hin*dIII. To a solution of pEGFP-C2 DNA (5 μL) was added a solution of **1** (5 μL) in various concentrations. All the samples were kept in the dark for 1 h at room temperature and then were incubated with *Hin*dIII (TaKaRa Biotechnology (Dalian) Co. Ltd.) according to the instructions provided by the supplier. After 15 min, loading buffer (TaKaRa Biotechnology (Dalian) Co. Ltd.) was added to stop enzyme reactions, and samples were then loaded into agarose gel. Free DNA and *Hin*dIII-digested free DNA were also applied on the gel as controls.

Inhibition of Topoisomerase I. To a solution of pEGFP-C2 DNA (5 μL) was added a solution of **1** (5 μL) in various concentrations. All the samples were kept in the dark for 1 h at room temperature and then were incubated with topoisomerase I (TaKaRa Biotechnology (Dalian) Co. Ltd.) according to the instructions provided by the supplier. After 15 min, the loading buffer was added to stop reactions, and samples were then loaded into the agarose gel. Free DNA and topoisomerase I-digested free DNA were also applied on the gel as controls.

DNA Translocation. 293T cells were routinely cultured in Dulbecco's Modified Eagle Medium (DMEM Gibco) supplemented with 10% (v/v) heat-inactivated fetal bovine serum and were seeded in a 24-well plate for 24 h to make sure that the cell covered 70% of the plate surface. The DNA/**1** complexes were prepared by mixing 2.2 μg of DNA and 135 mg of **1** in 100 μL of phosphate-buffered saline (PBS) buffer solution. The negative control was made by adding 135 mg of **1** directly in 100 μL of PBS solution. All the samples and control were incubated under room temperature for 1 h. Before translocation, the cell culture medium was taken out. The 100 μL PBS solution was then gently dripped into the cell wells. A further 400 μL of DMEM without serum was supplemented into each cell well. The cells were incubated in 5% CO_2 at 37 °C for 4 h and then supplemented with 500 μL of DMEM containing 20% heat-inactivated fetal bovine serum for a further 48 h incubation. The results were observed under a TE 2000-U fluorescent microscope (Nikon Japan) equipped with Spot software using an excitation wavelength of 420–490 nm.

Acknowledgment. This work was supported by 973 program (2006CB932900), NNSFC (90306009, 90403140, and 20421202), Tianjin Natural Science Foundation (TJ043801111 and 06YFJMJC04400), and Key Project of Chinese Ministry of Education (No. 107026), which are gratefully acknowledged.

REFERENCES AND NOTES

1. Balzani, V.; Ceroni, P.; Juris, A.; Venturi, M.; Puntariero, F.; Campagna, S.; Serroni, S. Dendrimers Based on Photoactive Metal Complexes. Recent Advances. *Coord. Chem. Rev.* **2001**, *219*, 545–572.
2. Beyeler, A.; Belser, P. Synthesis of a Novel Rigid Molecule Family for the Investigation of Electron and Energy Transfer. *Coord. Chem. Rev.* **2002**, *230*, 28–38.
3. Campagna, S.; Pietro, P. D.; Loiseau, F.; Maubert, B.; McClenaghan, N.; Passalacqua, R.; Puntoriero, F.; Ricevuto, V.; Serroni, S. Recent Advances in Luminescent Polymetallic Dendrimers Containing the 2,3-Bis(2′-pyridyl)pyrazine Bridging Ligand. *Coord. Chem. Rev.* **2002**, *229*, 67–74.
4. Demadis, K. D.; Hartshorn, C. M.; Meyer, T. J. The Localized-to-Delocalized Transition in Mixed-Valence Chemistry. *Chem. Rev.* **2001**, *101*, 2655–2685.

5. Brunschwig, B. S.; Creutz, C.; Sutin, N. Optical Transitions of Symmetrical Mixed-Valence Systems in the Class II-III Transition Regime. *Chem. Soc. Rev.* **2002**, *31*, 168–184.
6. Dam-Rauer, N. H.; Cerullo, G.; Yeh, A.; Boussie, T. R.; Shank, C. V.; McCusker, J. K. Femtosecond Dynamics of Excited-State Evolution in $[Ru(bpy)_3]^{2+}$. *Science* **1997**, *275*, 54–57.
7. Balzani, V.; Juris, A.; Venturi, M.; Campagna, S.; Serroni, S. Luminescent and Redox-Active Polynuclear Transition Metal Complexes. *Chem. Rev.* **1996**, *96*, 759–833.
8. Bargiletti, F.; Flamigni, L. Photoactive Molecular Wires Based on Metal Complexes. *Chem. Soc. Rev.* **2000**, *29*, 1–12.
9. Steiner, T. The Hydrogen Bond in the Solid State. *Angew. Chem., Int. Ed.* **2002**, *41*, 48–76.
10. Erkkila, K. E.; Odom, D. T.; Barton, J. K. Recognition and Reaction of Metallointercalators with DNA. *Chem. Rev.* **1999**, *99*, 2777–2796.
11. Sharma, S.; Chandra, M.; Pandey, D. S. New Multifunctional Complexes $[Ru(\kappa^3\text{-}L)(EPh_3)_2Cl]^+$ [E = P, As; L = 2,4,6-tris(2-pyridyl)-1,3,5-triazine] Containing both Group V and Polypyridyl Ligands. *Eur. J. Inorg. Chem.* **2004**, 3555–3563.
12. Ambroise, A.; Maiya, B. G. Ruthenium(II) Complexes of Redox-Related, Modified Dipyridophenazine Ligands: Synthesis, Characterization, and DNA Interaction. *Inorg. Chem.* **2000**, *39*, 4256–4263.
13. Mitra, D.; Di Cesare, N.; Sleiman, H. F. Self-Assembly of Cyclic Metal–DNA Nanostructures Using Ruthenium Tris(bipyridine)-Branched Oligonucleotides. *Angew. Chem., Int. Ed.* **2004**, *43*, 5804–5808.
14. Stewart, K. M.; Rojo, J.; McLaughlin, L. W. Ru(II) Tris(bipyridyl) Complexes with Six Oligonucleotide Arms as Precursors for the Generation of Supramolecular Assemblies. *Angew. Chem., Int. Ed.* **2004**, *43*, 5808–5811.
15. Liu, Y.; Chouai, A.; Degtyareva, N. N.; Lutterman, D. A.; Dunbar, K. R.; Turro, C. Chemical Control of the DNA Light Switch: Cycling the Switch ON and OFF. *J. Am. Chem. Soc.* **2005**, *127*, 10796–10797.
16. Connors, K. A. The Stability of Cyclodextrin Complexes in Solution. *Chem. Rev.* **1997**, *97*, 1325–1357.
17. Stella, V. J.; Rajewaki, R. A. Cyclodextrins: Their Future in Drug Formulation and Delivery. *Pharm. Res.* **1997**, *14*, 556–567.
18. Uekama, K.; Hirayama, F.; Irie, T. Cyclodextrin Drug Carrier Systems. *Chem. Rev.* **1998**, *98*, 2045–2076.
19. Loftssona, T.; Järvinen, T. Cyclodextrins in Ophthalmic Drug Delivery. *Adv. Drug Delivery Rev.* **1999**, *36*, 59–79.
20. Kumar, C. V.; Asuncion, E. H. Sequence Dependent Energy Transfer from DNA to a Simple Aromatic Chromophore. *Chem. Commun.* **1992**, 470–472.
21. Kumar, C. V.; Asuncion, E. H. DNA Binding Studies and Site Selective Fluorescence Sensitization of an Anthryl Probe. *J. Am. Chem. Soc.* **1993**, *115*, 8547–8553.
22. Ikeda, T.; Yoshida, K.; Schneider, H.-J. Anthryl(alkylamino)cyclodextrin Complexes as Chemically Switched DNA Intercalators. *J. Am. Chem. Soc.* **1995**, *117*, 1453–1454.
23. Nakanishi, K.; Berova, N.; Woody, R. W. *Circular Dichroism: Principles and Applications*; VCH: New York, 1994.
24. Rodger, A.; Nordén, B. *Circular Dichroism and Linear Dichroism*; Oxford University Press: New York, 1997.
25. Kajtar, M.; Horvath, T. C.; Kuthi, E.; Szejtli, J. A Simple Rule for Predicting Circular Dichroism Induced in Aromatic Guests by Cyclodextrin Hosts in Inclusion Complexes. *Acta Chim. Acad. Sci. Hung.* **1982**, *110*, 327–355.
26. Kodaka, M. A General Rule for Circular Dichroism Induced by a Chiral acrocycle. *J. Am. Chem. Soc.* **1993**, *115*, 3702–3705.
27. Shi, W.-X.; Larson, R. G. Atomic Force Microscopic Study of Aggregation of RecA-DNA Nucleoprotein Filaments into Left-Handed Supercoiled Bundles. *Nano Lett.* **2005**, *5*, 2476–2481.
28. Lin, Z.; Wang, C.; Feng, X.; Liu, M.; Li, J.; Bai, C. The observation of the local ordering characteristics of spermidine-condensed DNA: atomic force microscopy and polarizing microscopy studies. *Nucleic Acids Res.* **1998**, *26*, 3228–3234.
29. Wang, J. C. DNA Topoisomerases: Why So Many. *J. Biol. Chem.* **1991**, *266*, 6659–6662.
30. Liu, T.; Duan, Z.-Y.; Chen, L.; Feng, X.-Z. Non-viral Gene Delivery Carrier of Probe Type Host Molecule—Interactions Between DNA and β-cylodextrin Derivative Complexes (I). *Chin. Sci. Bull.* **2006**, *51*, 530–535.
31. Sullivan, B. P.; Salmon, D. J.; Meyer, T. J. Mixed Phosphine 2,2′-Bipyridine Complexes of Ruthenium. *Inorg. Chem.* **1978**, *17*, 3334–3341.